Aluminium oxide barrier films on polymeric web and their conversion for packaging applications

C. F. Struller[a, b], P. J. Kelly[a], N. J. Copeland[b], V. Tobin[c], H. E. Assender[c], C. W. Holliday[d], S. J. Read[d]

[a]Surface Engineering Group, Manchester Metropolitan University, Manchester, M1 5GD, UK

[b]Bobst Manchester Ltd., Pilsworth Road, Heywood, Lancashire OL10 2TL, UK

[c]Department of Materials, University of Oxford, Begbroke Science Park, Oxford OX5 1PF, UK

[d]Innovia Films Ltd., Lowther R&D Building, West Road, Wigton, Cumbria, CA7 9XX, UK

Corresponding author: Peter Kelly, Head of Surface Engineering Group, Dalton Research Institute, Manchester Metropolitan University, John Dalton Building, Chester Street, Manchester M1 5GD, Phone: +44 (0)161 247 4643, email: peter.kelly@mmu.ac.uk

ABSTRACT

In recent years, inorganic transparent barrier layers such as aluminium oxide or silicon oxide deposited onto polymer films have emerged as an attractive alternative to polymer based transparent barrier layers for flexible food packaging materials. For this application, barrier properties against water vapour and oxygen are critical. Aluminium oxide coatings can provide good barrier levels at thicknesses in the nanometre range compared to several micrometres for polymer-based barrier layer. These ceramic barrier coatings are now being produced on a large scale using industrial high speed vacuum deposition techniques, here, reactive evaporation on a ‘boat-type’ roll-to-roll metalliser. For the thin barrier layer to be useful in its final packaging application, it needs to be protected. This can be either via lamination or via an additional top coat. This study reports on acrylate topcoats, but also

undercoats on aluminium oxide coated biaxially oriented polypropylene films. The effect of the acrylate layer on barrier levels and surface topography and roughness was investigated. The acrylate was found to smooth the substrate surface and, as a top coat, to significantly improve barrier properties. Furthermore, the activation energy for water vapour and oxygen permeation was determined in order to investigate barrier mechanisms. The oxide coated film was, additionally, converted via adhesive lamination, which also provided improvement in barrier levels.

Keywords: Aluminium oxide, BOPP, barrier coatings, reactive evaporation, lamination, acrylate coatings

1. Introduction

Transparent barrier films have been attracting increasing interest in recent years. Applications range from moderate barrier levels required for food packaging to very high barrier levels for encapsulating electronic devices. With the transparent barrier flexible packaging market still growing worldwide at a rate of 10 to 15 % per year [1], the use of vacuum deposition techniques to produce transparent barrier layers such as aluminium oxide (AlO_x) or silicon oxide has become a favourable and powerful tool. For food packaging, this market is traditionally dominated by ethylene vinyl alcohol copolymer co-extruded barrier layer films and polyvinylidene chloride coated films [2]. However, vacuum-deposited barrier coatings only require a small fraction of the thickness of these barrier layers, i.e. their thickness is three orders of magnitude smaller, whilst still producing comparable barrier properties. The standard aluminium metallisation process, usually carried out in a roll-to-roll coater, can be modified by the injection of oxygen into the aluminium vapour in order to deposit a transparent aluminium oxide barrier layer; a process that has been developed over the last few decades [3-7]. The use of such large scale and high speed coating equipment can potentially

provide vast economic and environmental benefits, which is of great importance for the low cost packaging market where profit margins generally are small. There is, though, a further conversion step required in order to obtain the final packaging structure. This is either achieved by laminating the vacuum coated films (adhesive lamination, extrusion lamination) or via application of an additional polymer coating on top of the inorganic layer, both serving the purpose of protecting the thin barrier layer during its final packaging application. In the course of this investigation, the effects of adhesive lamination as well as acrylate coatings on AlO_x coated polymer film was examined.

2. Experimental

2.1. Substrate, coating and conversion processes

The film used in this study was a 20 µm thick three layer coextruded biaxially oriented polypropylene (BOPP) film with a homopolymer core and either a co- or terpolymer skin layer on each side. The film was also corona treated in-house by the film manufacturer. The corona treated side was coated with a 10 nm thin AlO_x layer via reactive thermal evaporation on an industrial roll-to-roll metalliser using a Bobst Manchester (formerly General Vacuum Equipment) General K4000 vacuum metalliser. This vacuum coater has a source consisting of resistively heated evaporation boats onto which aluminium wire is continuously fed. Oxygen is introduced into the aluminium vapour cloud to produce a transparent aluminium oxide coating and an optical monitoring beam and closed loop control system is used to achieve consistent optical properties of the coated film across the web width and length. The pressure during aluminium oxide deposition is of the order of 0.1 Pa. AlO_x layers were deposited onto rolls of film (for acrylate top coats and lamination) and A4 samples mounted onto a carrier web (for acrylate undercoats).

The acrylate deposition was achieved via flash evaporation of a monomer liquid in vacuum. These monomers condense as a liquid film on the substrate surface and are subsequently cured using electron beam radiation (with a current of 400 mA) to obtain a cross-linked layer. Acrylate deposition was carried out on a system licensed by Sigma Technologies International Inc. (USA). Tripropylene glycol diacrylate was chosen as a monomer and an acrylate thickness of 0.75 µm was deposited. Acrylate layers were coated onto A4 samples as undercoats and topcoats prior and after AlO_x deposition as an off-line process.

Lamination of the AlOx coated film was performed on an industrial laminator (Bobst Rotomec CL850) via solvent-based adhesive lamination. A high performance two component polyurethane adhesive was used and the AlO_x coated BOPP was laminated against another plain 20 µm BOPP film.

2.2. Analytical methods

Oxygen and water vapour transmission rates (OTR/WVTR) were determined in compliance with ASTM F 1927 and ASTM F 1249/ISO 15106-3 using a Mocon Oxtran 2/20 and Systech Illinois 8001 for oxygen permeation and a Mocon Permatran-W 33/3 and Systech Illinois 7001 for water vapour permeation. Test conditions for OTR were 23 °C and 50 % relative humidity (RH), whilst WVTR is stated for 38 °C and a gradient of 90 % RH. During WVTR measurement of coated samples, the coated side was always facing the 0 % RH. For the determination of the apparent activation energy of oxygen/moisture permeation, barrier measurements were carried out at 4 different temperatures (20 °C, 30 °C, 40 °C in addition to the respective temperature for a standard measurement).

A Veeco DI CP II atomic force microscope (AFM) in tapping mode was used to acquire roughness data and topography images. All images were corrected by first order line-wise levelling. Root mean square (RMS) values were calculated from 5 x 5 μm^2 size scans.

3. Results and discussion

3.1. Acrylate coated films

3.1.1 Barrier performance

The barrier performance of AlO_x coated BOPP with and without the application of acrylate top- and undercoats is summarised in *Table I*. Additionally, the barrier properties of the plain BOPP film and the acrylate coated BOPP film prior to AlO_x deposition are listed. As can be seen, the OTR of the plain film can be significantly reduced by the application of the inorganic AlO_x layer. Nevertheless, the improvement of WVTR is only marginal. These differences have been attributed to the film surface properties affecting coating nucleation and growth and thus the final structure of the thin AlO_x barrier layer [7, 8]. Furthermore, the use of an acrylate undercoat prior to AlO_x deposition can additionally enhance the oxygen as well as water barrier, though the acrylate on its own only slightly improves the plain film OTR and leaves the WVTR unchanged. This has also been reported by other research groups for AlO_x layers on polypropylene [9] and polyethylene terephthalate [10-13] and is assigned to a variety of changes the acrylate confers to the polymer film. Acrylate layers have the capability to smoothen the substrate surface, eliminate surface features and thus decouple its defects from the subsequently deposited inorganic barrier layer [10, 12-15]. Furthermore, the barrier properties of the acrylate itself, which has a better oxygen barrier than BOPP [16], play a role, as this can affect and reduce the concentration gradient of the permeating substance in the polymer layer adjacent to the defect [17, 18]. Finally, the acrylate represents a change of surface chemistry which may offer more nucleation sites to the depositing

inorganic coating thus resulting in a denser coating structure [9, 12]. The improvement seen when applying an acrylate topcoat, especially the significant enhancement of WVTR to less than 1 g/(m² d), has been attributed to the infiltration of the acrylate into the defects of the AlO_x layer ('pore-filling') [19, 20] and therefore the reduction of the permeation coefficient within the defects from that of air to that of the acrylate. A protection of the barrier layer by the topcoat from damage during winding and handling, which is generally argued to be the reason for the barrier improvement [9, 10], can be excluded in our case as the acrylate was not applied in-line, but as an off-line solution with the AlO_x coated samples being rewound in vacuum as well as being handled prior to depositing the topcoat. Additionally, as stated for the undercoat, the permeability properties of the acrylate are of importance in improving the barrier properties.

3.1.2 Apparent activation energy

To further investigate the permeation mechanisms of oxygen and moisture through AlO_x coated and acrylate topcoated, films the activated rate theory was applied in order to calculate apparent activation energies of permeation [21-23]. The Arrhenius plots of this investigation and the activation energies obtained are summarised in *Fig. 1* and *Table II*, respectively. As can be seen, the activation energy of oxygen permeation remains largely unchanged by the application of the AlO_x layer as well as the acrylate topcoat, which indicates a macro-defect dominated permeation of oxygen through the coated film with the permeation through the BOPP polymer being the rate limiting step [24]. Furthermore, the activation energies obtained for oxygen are in agreement with values given in the literature [24-26]. For water vapour the AlO_x layer apparently slightly decreases the activation energy, whilst the application of the acrylate topcoat results in an increase back to the level of plain BOPP. It is, however assumed, that this change is not significant given the relatively small number of

samples tested; in this case two (compare also high standard deviations of activation energies obtained by Tropsha and Harvey [21]). The lack of significant change in activation energy is attributed to a macro-defect driven mechanism, as stated previously for oxygen permeation. There are, however, also a few cases published where despite the unchanged activation energy additional investigations suggested a chemical interaction rather than a defect dominated permeation [21, 27]. The activation energy values for water vapour permeation through uncoated BOPP fall within the broad range of values reported in literature (Deng et al. [24] 64.6 ± 2.0 kJ/mol, Tropsha and Harvey [21] 38.9 ± 2.1 kJ/mol).

3.1.3 Surface topography

The surface topographies of the uncoated and acrylate undercoated films were additionally investigated. Differential interference contrast light microscopy (no images shown Thin solid films does not accept supplementary data) revealed major changes induced by the acrylate with smaller filler particles being masked by the acrylate layer as well as the typical BOPP film texture (‘orange-peel’) being eliminated, which is in agreement with results published by other researchers [10, 14, 28]. AFM investigation of the uncoated and acrylate coated BOPP revealed a substantial decline of surface roughness with RMS values decreasing from 4.1 ± 0.3 nm to 1.1 ± 0.1 nm by the application of the acrylate layer, accompanied by a considerable change in surface structure, as can be seen in *Fig. 2*. The acrylate RMS roughness compares well with a range of 0.8 to 1.5 nm as stated by Affinito et al. [11].

3.2. Lamination

For the industrial scale lamination two trials were conducted. Firstly, the adhesive was applied onto the uncoated BOPP, which was then laminated against the AlO_x coated film. In the second trial, the adhesive was applied onto the AlO_x layer itself and subsequently the

AlO_x coated film was combined with the plain BOPP. In both cases, the AlO_x barrier layer is embedded between and protected by the BOPP films and is adjacent to the adhesive layer. As can be seen from the barrier performance pre and post lamination stated in *Table III*, the OTR could be significantly decreased, whilst WVTR was approximately halved. The latter is due to doubling the thickness of the film by adding another 20 µm thick BOPP. The improvement of OTR is assigned to the barrier properties of the adhesive (lower oxygen permeability compared to BOPP) and the resulting reduction of the concentration gradient in the adhesive layer adjacent to the defects [29]. Furthermore, the infiltration of the adhesive into defects in the AlO_x layer [30], as discussed for the acrylate topcoat, can play an important role. This was, though, only the case when the adhesive was applied onto the uncoated BOPP. When the adhesive was applied onto the AlO_x layer, the OTR was increased indicating damage (mechanical or chemical) to the thin coating. The compatibility of the AlO_x coating with the adhesive and solvent was tested on samples taken of the AlO_x coated BOPP prior to lamination and no barrier deterioration was detected. Hence, a chemical attack of the AlO_x by either the solvent or the adhesive is excluded and a mechanical nature of the damage during adhesive application or drying (solvent removal) is assumed to be the reason for the barrier loss during lamination trial two.

4. Summary and conclusions

Acrylate top- and undercoats as well as adhesive lamination can significantly enhance the barrier performance of reactively evaporated AlO_x barrier layers on BOPP film. The change of surface chemistry and the smoothing of the BOPP film surface induced by the acrylate undercoat are thought to be of major importance for this barrier enhancement. During topcoating and presumably also lamination, the infiltration of the acrylate and adhesive into defects of the inorganic AlO_x layer, such as cracks, pinholes or pores, and the better oxygen

barrier properties of the acrylate/adhesive can account for the obtained improvement of barrier levels. The investigation of apparent activation energy revealed a macro-defect driven permeation process through the AlO_x coated as well as acrylate topcoated film for both, oxygen and water vapour.

References

[1] C.A. Bishop, Roll-to-roll vacuum deposition of barrier coatings, Scrivener, Salem, 2010.

[2] The future of transparent barrier films to 2011, Pira International Ltd., Leatherhead, 2006.

[3] R.S.A. Kelly, 36th Annual Technical Conference Proceedings of the Society of Vacuum Coaters, 1993, p. 312.

[4] R.S.A. Kelly, 37th Annual Technical Conference Proceedings of the Society of Vacuum Coaters, 1994, p. 144.

[5] S. Schiller, M. Neumann, H. Morgner, N. Schiller, 37th Annual Technical Conference Proceedings of the Society of Vacuum Coaters, 1994, p. 203.

[6] S. Günther, S. Straach, N. Schiller, A.L. Quiceno, A.G. Contreras, R. Ludwig, G. Hoffmann, 52nd Annual Technical Conference Proceedings of the Society of Vacuum Coaters, 2009, p. 727.

[7] C.F. Struller, P.J. Kelly, N.J. Copeland, C.M. Liauw, J. Vac. Sci. Technol. A 30 (4) (2012) 041502.

[8] C.F. Struller, P.J. Kelly, N.J. Copeland, C.M. Liauw, AIMCAL Fall Technical Conference. Myrtle Beach, USA, 2012.

[9] A. Yializis, 38th Annual Technical Conference Proceedings of the Society of Vacuum Coaters, 1995, p. 95.

[10] J.D. Affinito, M.E. Gross, C.A. Coronado, G.L. Graff, I.N. Greenwell, P.M. Martin, Thin Solid Films 290–291 (1996) 63.

[11] J.D. Affinito, S. Eufinger, M.E. Gross, G.L. Graff, P.M. Martin, Thin Solid Films 308–309 (1997) 19.

[12] T. Miyamoto, K. Mizuno, N. Noguchi, T. Niijima, 44th Annual Technical Conference Proceedings of the Society of Vacuum Coaters, 2001, p. 166.

[13] G.L. Graff, R.E. Williford, P.E. Burrows, J. Appl. Phys. 96 (4) (2004) 1840.

[14] A. Yializis, M.G. Mikhael, R.E. Ellwanger, 43rd Annual Technical Conference Proceedings of the Society of Vacuum Coaters, 2000, p. 404.

[15] A.G. Erlat, B.M. Henry, C.R.M. Grovenor, A.G.D. Briggs, R.J. Chater, Y. Tsukahara, J. Phys. Chem. B 108 (3) (2004) 883.

[16] M. Hanika, H.-C. Langowski, U. Moosheimer, 45th Annual Technical Conference Proceedings of the Society of Vacuum Coaters, 2002, p. 519.

[17] E.H.H. Jamieson, A.H. Windle, J. Mater. Sci. 18 (1) (1983) 64.

[18] T.A. Beu, P.V. Mercea, Mater. Chem. Phys. 26 (3-4) (1990) 309.

[19] J.D. Affinito, D. Hilliard, 47th Annual Technical Conference Proceedings of the Society of Vacuum Coaters, 2004, p. 563.

[20] G. Aresta, J. Palmans, M.C.M. van de Sanden, M. Creatore, Microporous and Mesoporous Mater. 151 (2012) 434.

[21] Y.G. Tropsha, N.G. Harvey, J. Phys. Chem. B 101 (13) (1997) 2259.

[22] A.G. Erlat, R.J. Spontak, R.P. Clarke, T.C. Robinson, P.D. Haaland, Y. Tropsha, N.G. Harvey, E.A. Vogler, J. Phys. Chem. B 103 (29) (1999) 6047.

[23] A.P. Roberts, B.M. Henry, A.P. Sutton, C.R.M. Grovenor, G.A.D. Briggs, T. Miyamoto, M. Kano, Y. Tsukahara, M. Yanaka, J. Memb. Sci. 208 (1-2) (2002) 75.

[24] C.S. Deng, H.E. Assender, F. Dinelli, O.V. Kolosov, G.A.D. Briggs, T. Miyamoto, Y. Tsukahara, J. Polym. Sci. B Polym. Phys. 38 (23) (2000) 3151.

[25] S.-I. Hong, J.M. Krochta, J. Food. Eng. 77 (3) (2006) 739.

[26] M. Kurek, D. Klepac, M. Ščetar, K. Galić, S. Valić, Y. Liu, W. Yang, Polym. Bull. 67 (7) (2011) 1293.

[27] B.M. Henry, F. Dinelli, K.Y. Zhao, C.R.M. Grovenor, O.V. Kolosov, G.A.D. Briggs, A.P. Roberts, R.S. Kumar, R.P. Howson, Thin Solid Films 355-356 (1999) 500.

[28] B.M. Henry, D. Howells, J.A. Topping, H.E. Assender, C.R.M. Grovenor, L. Marras, 49th Annual Technical Conference Proceedings of the Society of Vacuum Coaters, 2006, p. 654.

[29] H.-C. Langowski, In: O.G. Piringer, A.L. Baner (Eds.), Plastic Packaging - Interactions with Food and Pharmaceuticals, Wiley-VCH, Weinheim, 2008, p. 297.

[30] O. Miesbauer, M. Schmidt, H.-C. Langowski, Vakuum in Forschung und Praxis 20 (2008) 32.

List of figure and table captions

Fig. 1: Arrhenius plots of ln(OTR), top, and ln(WVTR), bottom, as a function of 1/T for uncoated, AlO_x coated and acrylate topcoated BOPP.

Fig. 2: Representative 5 x 5 µm² AFM scans of uncoated BOPP (top) and acrylate coated BOPP, undercoat, no AlO_x (bottom).

Table I – Barrier performance of AlO_x coated BOPP in combination with acrylate top- and undercoats.

Table II – Apparent activation energy E_A of oxygen and water vapour permeation through uncoated BOPP, AlO_x coated BOPP and acrylate topcoated AlO_x coated BOPP.

Table III – Barrier performance of AlO_x coated BOPP before and after adhesive lamination.

Table I – Barrier performance of AlO_x coated BOPP in combination with acrylate top- and undercoats.

Description	**OTR**	**WVTR**
	$cm^3/(m^2\ d)$	**$g/(m^2\ d)$**
BOPP (uncoated)	≈ 2100	6 – 7
BOPP + *Acrylate undercoat*	1675.50 ± 129.40	6.59 ± 0.08
BOPP + *Acrylate undercoat* + AlO_x	15.83 ± 1.94	1.93 ± 0.21
BOPP + AlO_x	26.68 ± 3.07	4.73 ± 0.07
BOPP + AlO_x + *Acrylate topcoat*	13.65 ± 0.49	0.46 ± 0.07

Table II – Apparent activation energy E_A of oxygen and water vapour permeation through uncoated BOPP, AlO_x coated BOPP and acrylate topcoated AlO_x coated BOPP.

Description	**E_A (OTR)**	**E_A (WVTR)**
	kJ/mol	**kJ/mol**
BOPP (uncoated)	41.5 ± 0.3	57.3 ± 0.2
BOPP + AlO_x	39.4 ± 0.3	51.8 ± 0.4
BOPP + AlO_x + *Acrylate topcoat*	39.2 ± 0.7	58.6 ± 1.1

Table III – Barrier performance of AlO_x coated BOPP before and after adhesive lamination.

Description	**OTR**	**WVTR**
	$cm^3/(m^2\ d)$	**$g/(m^2\ d)$**
BOPP + AlO_x (before lamination)	48.62 ± 8.18	4.76 ± 0.35
Lamination 1: adhesive onto uncoated BOPP	11.92 ± 0.61	2.63 ± 0.17
Lamination 2: adhesive onto AlO_x	183.05 ± 6.87	2.81 ± 0.08

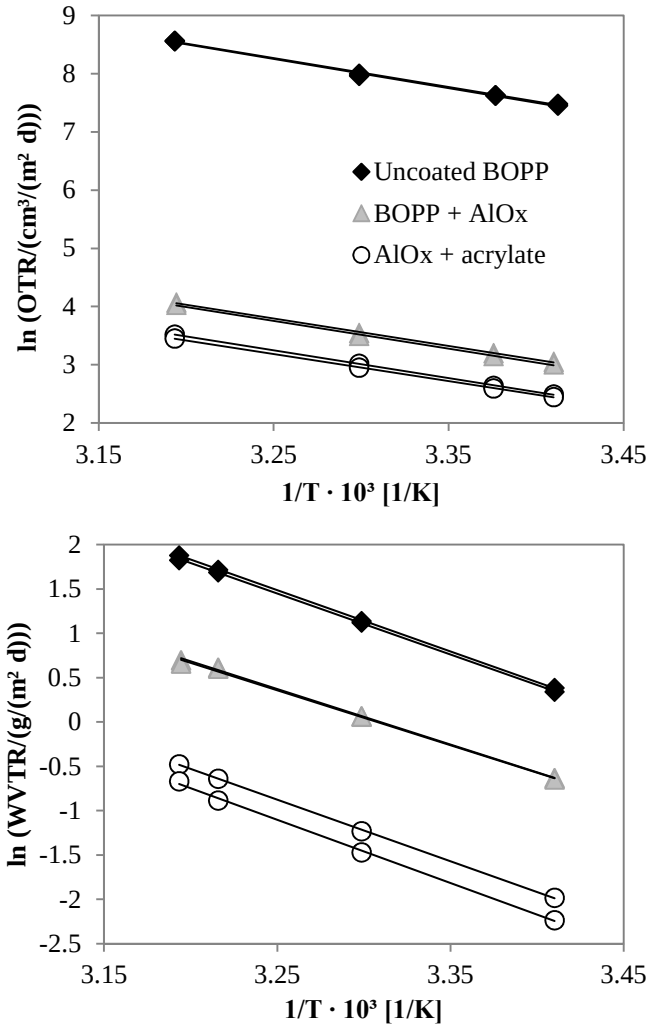

Fig. 1: Arrhenius plots of ln(OTR), top, and ln(WVTR), bottom, as a function of 1/T for uncoated, AlO_x coated and acrylate topcoated BOPP

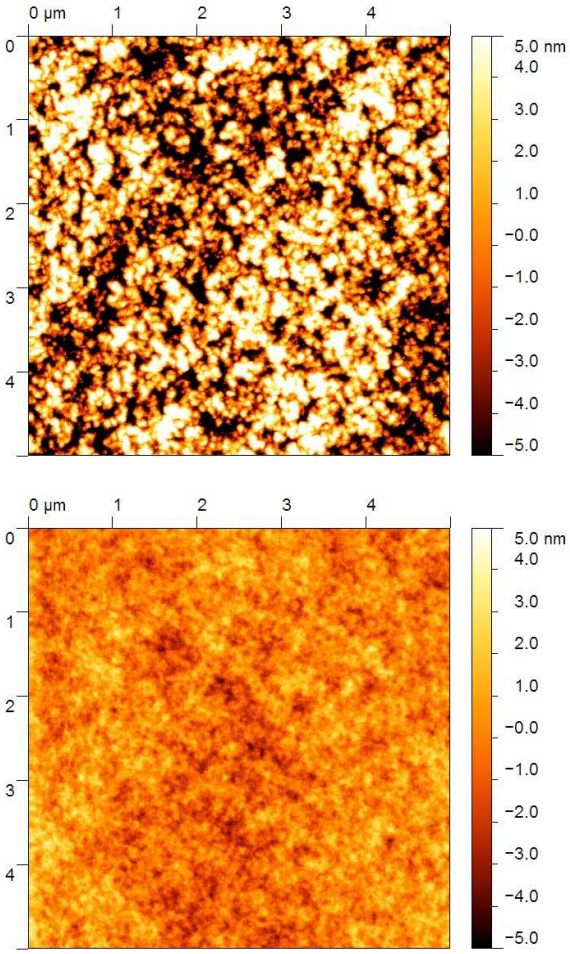

Fig. 2: Representative 5 x 5 µm² AFM scans of uncoated BOPP (top) and acrylate coated BOPP (undercoat no AlO_x, bottom)